

Instability of a polymeric thread

J. Eggers

*School of Mathematics, University of Bristol, University Walk, Bristol BS8 1TW,
United Kingdom*

(Received 12 August 2013; accepted 17 March 2014; published online 31 March 2014)

When a liquid containing a dilute solution of long, flexible polymers breaks up under the action of surface tension, it forms long threads of nearly uniform thickness. However, at a thickness in the order of microns, the thread becomes unstable to the formation of a non-uniform “blistering” pattern: tiny drops separated by threads of highly concentrated polymer solution. We show that standard models for the coupling between stress and polymer concentration lead to a linear instability, which exhibits very strong transient growth of the free surface perturbation. A high concentration of polymer remains in the thread part of the structure. © 2014 AIP Publishing LLC. [<http://dx.doi.org/10.1063/1.4869721>]

I. INTRODUCTION

The breakup of a piece of fluid is affected strongly by the presence of long, flexible polymers dissolved in it. In the case of a Newtonian fluid, pinch-off is described by localized similarity solutions, leading to breakup in finite time.^{2,3} However, even a small amount of polymer leads to the formation of thin threads of uniform thickness,⁴⁻⁷ and breakup is inhibited. The reason is that polymers are stretched in the extensional flow close to the pinch point, leading to a buildup of elastic stresses. The rate of thinning $\dot{\epsilon}$ of the fluid neck is now controlled by the rate at which polymers can relax, determined in the simplest case by the inverse of the polymer time scale λ . This means the filament thins exponentially as polymers are stretched, and the finite-time pinch-off singularity is regularized.

However, once the polymeric thread has become sufficiently thin, it is observed to be subject to instabilities (“blistering”),^{1,8,9} which destroy its uniformity. A variety of different instabilities has been reported,⁹ but here we focus on the growth of sinusoidal perturbations, which grow exponentially,¹ indicating a linear instability. In Fig. 1, we show both the initial stage of exponential growth, which lasts for about 10 ms (first five profiles), as well as the later, nonlinear stages of the instability. In this paper, we will be concerned with the linear part of the instability only. One observes a rapid growth of perturbations, on a time scale much shorter than that on which thinning of the thread takes place.

A possible explanation for this instability is that polymers have become fully stretched,⁶ so that the extensional viscosity has reached a plateau value. The dynamics should thus resemble that of a Newtonian fluid, which is susceptible to the Rayleigh instability.³ However, numerical simulations using the FENE-P model, which incorporates finite extensibility of polymer molecules, show that this situation leads to localized pinch-off,¹⁰ rather than a sinusoidal instability. Moreover, it was shown in Refs. 1 and 9 that the growth rate of the observed blistering instability is much greater than that expected for a Newtonian fluid of the corresponding extensional viscosity. In, Ref. 11, an iterated local instability of a polymeric thread is described on the basis of the Oldroyd B model,¹² which assumes infinite extensibility. However, the calculation does not predict a spatially periodic structure such as that shown in Fig. 1. Another mechanism for the formation of beads that has been proposed^{10,13} requires the presence of inertia, a remnant of the initial dynamics; at least for the experiments considered in Refs. 1 and 9, inertia was shown not to play a role. In addition, inertia does not explain the formation of a periodic structure.

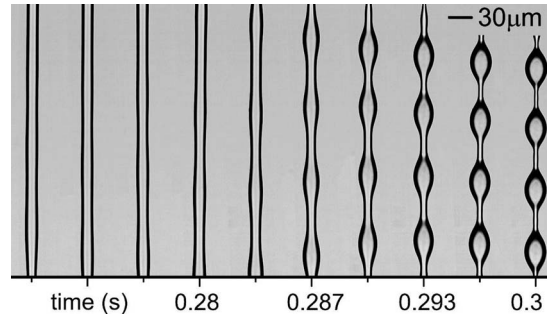


FIG. 1. Growth of a sinusoidal instability on a viscoelastic filament; the spacing of the pictures is 300^{-1} s.¹ The inverse growth rate is $\omega^{-1} = 9.3$ ms, while the time scale of thinning is $\epsilon^{-1} = 130$ ms. Exponential growth is observed for the first 10 ms (the first five profiles).

Here we propose that the origin of the instability comes from the coupling between the polymeric stress σ and the polymer density n ,¹⁴ driving a non-uniform polymer concentration. Indeed, it has been observed that the polymer concentration along the thread becomes highly non-uniform,¹ indicating that a coupling to the polymer density has to be included in the modeling in order to explain the effect. The idea of a stress-density coupling has previously been applied to light scattering data for both shear and extensional flow,¹⁵⁻¹⁷ as well as anomalous slip lengths in shear flow¹⁸ and shear banding.¹⁹ The origin of the instability lies in the flow of polymers toward regions of high stress, i.e., highly extended polymers. This flux leads to further extension, fueling an instability.

II. POLYMER MODEL

To insure a consistent framework, we will base our calculations on model equations for dilute polymer solutions near equilibrium. The polymers are modeled as elastic Hookean dumbbells.¹² In many pinching experiments, the concentration is semi-dilute, and in particular, polymers have reached a highly stretched state. Owing to these effects, transport coefficients may well be renormalized significantly, but we expect the structure of the equations to be robust.

Equations for the polymer density and the stress have been developed for an elastic Hookean dumbbell model by Bhawe *et al.*¹⁸ and by Öttinger,²⁰ with slightly different results. Both sets of equations have been reviewed in Ref. 21, and have been found to agree, if one drops consistently terms quadratic in the stress and of third order in the gradients. For the number density of polymers, one obtains the diffusion equation

$$\frac{Dn}{Dt} = -\frac{D}{k_B T} \nabla \nabla : \sigma_p + D \Delta n, \quad (1)$$

where the convected (substantial) derivative appears on the left, and D is the diffusion constant of a polymer strand; σ_p is the polymeric contribution to the fluid stress. The first term on the right of (1) describes the entropically driven flow of particles toward regions of high polymer extension, i.e., a more ordered state, the second term describes the diffusion of polymer chains. Note that the diffusion coefficients in front of the first and second term on the right of (1) are the same.¹⁴ Equation (1) is Eq. (6) of Ref. 21 (with $\tau_p = -\sigma_p$), based on a Hookean dumbbell model. The same equation was found in Ref. 20, again analyzing a Hookean dumbbell, in the two-fluid description of Mavrantzas and Beris,²² and for a Rouse chain.²¹ In the original paper of Bhawe *et al.*,¹⁸ one additional term appeared on the right hand side of (1), but which was later found to be absent in a consistent formulation up to second order gradients.²¹

The equation of motion for the velocity field is the Navier-Stokes equation, but with an extra term accounting for the polymeric contribution to the stress:

$$\rho \frac{D\mathbf{v}}{Dt} = -\nabla p + \nabla \cdot \boldsymbol{\sigma}_p + \eta_s \Delta \mathbf{v}, \quad (2)$$

where η_s is the solvent contribution to the viscosity.

To close the set of equation, we need a constitutive equation for $\boldsymbol{\sigma}_p$, which is derived from the (stochastic) dynamics for the polymer conformations:

$$\frac{D\boldsymbol{\sigma}_p}{Dt} = (\nabla \mathbf{v})^T \cdot \boldsymbol{\sigma}_p + \boldsymbol{\sigma}_p \cdot (\nabla \mathbf{v}) - \frac{\boldsymbol{\sigma}_p}{\lambda} + nk_B T ((\nabla \mathbf{v})^T + (\nabla \mathbf{v})) - k_B T \frac{Dn}{Dt} \boldsymbol{\delta} + D\Delta \boldsymbol{\sigma}_p, \quad (3)$$

which is Eq. (51) of Ref. 18 and Eq. (3) of Ref. 21, derived for Hookean dumbbells. The first two terms on the right describe the deformation of polymers by the flow (“upper convected derivative”); in an extensional flow, this results in rapid stretching of polymer strands, and a strong increase in extensional viscosity. The next term comes from the relaxation of polymers toward an equilibrium (coiled) state, while the fourth term describes the diffusion of beads in the Hookean dumbbell model. From a balance between the third and fourth terms, one finds the polymeric contribution $\eta_p = n\lambda k_B T$ to the viscosity, valid near equilibrium. The fifth term, involving the substantial derivative of the polymer concentration, has the same origin than the fourth, and will prove crucial in coupling the polymer concentration to the flow field, balancing with the stretching term. Finally, stress is allowed to relax by diffusion, as described by the last term on the right-hand side of (3), introduced in Ref. 23.

In a liquid thread, we also have to couple to the motion of the free surface, and include driving by capillary forces. Since the thread we consider is long and slender, we confine ourselves to simplified description in which the flow and the stress distribution is assumed to be one-dimensional, and a standard calculation³ yields:

$$\dot{h} + v h_z = -v_z \frac{h}{2}, \quad (4)$$

$$\rho (\dot{v} + v v_z) = -\gamma \kappa_z + 3\eta_s \frac{1}{h^2} (h^2 v_z)_z + \frac{1}{h^2} (h^2 \sigma)_z, \quad (5)$$

$$\kappa = \frac{1}{h(1+h_z^2)^{3/2}} - \frac{h_{zz}}{(1+h_z^2)^{5/2}}, \quad (6)$$

$$\dot{\sigma} + v \sigma_z = 2v_z \sigma + 2nk_B T v_z - \frac{\sigma}{\lambda} - k_B T (\dot{n} + v n_z) + D\sigma_{zz}, \quad (7)$$

$$\dot{n} + v n_z = Dn_{zz} - \frac{D}{k_B T} \sigma_{zz}, \quad (8)$$

where $h(z, t)$ is the local thread radius, $v(z, t)$ the axial velocity, and $\sigma(z, t)$ the axial polymeric stress; we neglect the radial polymeric stress, which is small in an extensional situation. The subscript denotes differentiation with respect to the variable, and the dot denotes the time derivative. The first equation describes the deformation of the free surface by the flow, while the second is the one-dimensional version of the momentum balance (2), with κ being (twice) the mean curvature. The last two equations are the one-dimensional versions of (1) and (3), respectively.

We will consider the case that inertial effects are small, so the terms on the left of (5) can be neglected, and we can perform one spatial integration. As a result, there is a constant tension $T(t)$ in the fluid thread:⁷

$$h^2 (\gamma \kappa + 3\eta_s v_z + \sigma) = T(t), \quad (9)$$

where we have defined

$$K = \frac{1}{h(1+h_z^2)^{\frac{1}{2}}} + \frac{h_{zz}}{(1+h_z^2)^{\frac{3}{2}}}. \quad (10)$$

Note that K is *not* the mean curvature of the interface (which would have a $-$ sign in front of the second term).⁷ As explained in Ref. 7, (10) results from the total surface tension contribution to the tensile force T , which is composed of “bulk” stresses exerted over the cross-sectional area, and a line force exerted around the perimeter.

III. BASE SOLUTION

The model described so far leads to a uniform thread of highly stretched polymers which thins at a constant rate, described in detail in Ref. 7. Inside the thread there is an extensional flow

$$\bar{v} = 2\dot{\epsilon}z, \quad (11)$$

which causes fluid contained in the filament to empty into the drops, producing an elongational flow with elongation rate

$$\dot{\epsilon} = -\frac{\partial_t \bar{h}}{\bar{h}}. \quad (12)$$

As a result, polymers are being stretched by the flow at a rate $\dot{\epsilon}$, leading to exponential increase in the stress

$$\bar{\sigma} = \sigma_0 e^{\dot{\epsilon}t} \quad (13)$$

supported by the polymers. Throughout, we will be concerned with solvents of low viscosity, whose contribution to the total stress is negligible except at the very first stages of breakup, not considered here. On the other hand, the stress (13) is being balanced by the capillary pressure difference, which implies that the drop radius has to decrease like

$$\bar{h} = h_0 e^{-\dot{\epsilon}t}, \quad (14)$$

consistent with a constant $\dot{\epsilon}$, defined by (12). The value of $\dot{\epsilon}$ is set by the balance between stretching and polymer relaxation, which leads to⁴

$$\dot{\epsilon} = 1/(3\lambda).$$

Note, however, that in practice significant deviations between measured values of $\dot{\epsilon}$ and rheological measurements of λ have been reported,⁶ which may be the result of polydispersity,²⁴ or multiple time scales present on a single polymer chain.²⁵ Significant effects of polymer concentration on the stretch rate have been reported as well.²⁶

In Ref. 7, we use matching between the thread and the drops to show that the amplitudes h_0 and σ_0 are related by

$$\sigma_0 = \frac{f\gamma}{h_0}, \quad (15)$$

where $f=2$, and the tension in the thread is

$$T(t) = (1+2f)\gamma h_0 e^{-\dot{\epsilon}t}. \quad (16)$$

Our matching procedure did use a slender filament description for the transition region between thread and drop, where it is strictly speaking not valid. Therefore, it is possible that the value of f is somewhat different for the true three-dimensional model. For this reason we will perform some of the calculations below for general f . So far, the base solution we have described corresponds to a constant polymer concentration $n = \bar{n}$.

IV. PERTURBATION THEORY

Now we add a small perturbation the base solution described above, putting

$$h(z, t) = \bar{h} + h_0 \epsilon_1(t) \sin kz, \quad (17)$$

$$v_z(z, t) = \bar{v}_z + \dot{\epsilon} \epsilon_2(t) \sin kz, \quad (18)$$

$$\sigma(z, t) = \bar{\sigma} + \sigma_0 \epsilon_3(t) \sin kz, \quad (19)$$

$$n(z, t) = \bar{n} + \bar{n} \epsilon_4(t) \sin kz, \quad (20)$$

which makes all the amplitudes ϵ_i dimensionless. The effect of the mean flow field (11) is that perturbations become stretched, leading to an exponential increase in wavelength: the wavenumber k must be time dependent. Specifically, the equation of motion to be satisfied by k is

$$\frac{\dot{k}}{k} = -\frac{\bar{v}}{z} = -2\dot{\epsilon}, \quad (21)$$

with solution

$$k = k_0 e^{-2\dot{\epsilon}t}. \quad (22)$$

Note that the inverse growth rate of perturbations shown in Fig. 1 is short compared to the time scale of thinning, so that the change in wavelength during the linear part of the instability (about 10 ms) is less than 20%. Unfortunately, measurements of the wavelength are currently not sufficiently accurate to detect such a small change.⁹ We attribute the slight decrease in the wavelength of perturbations seen in the last five frames of Fig. 1 to nonlinear effects.

It is straightforward to check that if k is chosen according to (22) in (17)–(20), the extra term coming from the time derivative of k cancels against the convective terms on the left of (4)–(8). In the following, we neglect the contribution of the solvent viscosity η_s , since its contribution to the stress is very small compared to the polymeric stress.

Inserting (17), (18) into (4) and linearizing in ϵ_i , we find

$$\dot{\epsilon}_1 = -\frac{\dot{\epsilon} e^{-\dot{\epsilon}t}}{2} \epsilon_2 - \dot{\epsilon} \epsilon_1. \quad (23)$$

The linearized form of the force balance (9) reads

$$\epsilon_3 = \frac{e^{2\dot{\epsilon}t}}{2} \left(\bar{h}^2 k^2 - 1 - 2f \right) \epsilon_1, \quad (24)$$

where we have used (15). Next the constitutive Eq. (7) leads to

$$\dot{\epsilon}_3 = \dot{\epsilon} \epsilon_3 + \frac{\dot{\epsilon}}{\sigma_0} (2\sigma_0 e^{\dot{\epsilon}t} + 2\bar{n}k_B T) \epsilon_2 + 4 \frac{\dot{\epsilon}}{\sigma_0} \bar{n}k_B T \epsilon_4 - \frac{\bar{n}k_B T}{\sigma_0} \dot{\epsilon}_4 - Dk^2 \epsilon_3, \quad (25)$$

having used $1/\lambda = 3\dot{\epsilon}$. Finally, the linearized version of (8) is

$$\dot{\epsilon}_4 = \frac{D\sigma_0}{\bar{n}k_B T} k^2 \epsilon_3 - Dk^2 \epsilon_4. \quad (26)$$

With the help of (23) and (24), we can eliminate ϵ_2 and ϵ_3 . We also introduce the dimensionless time $\tau = \dot{\epsilon}t$ and dimensionless initial wave number $p_0 = h_0 k_0$. As a result, (25) and (26) turn into the linear system

$$\frac{d\epsilon_1}{d\tau} = a(\tau)\epsilon_1 + b(\tau)\epsilon_4, \quad \frac{d\epsilon_4}{d\tau} = c(\tau)\epsilon_1 + d(\tau)\epsilon_4, \quad (27)$$

with

$$\begin{aligned} a(\tau) &= [1 - 2f + 5p_0^2 e^{-6\tau} - 4Ne^{-\tau} + 2\bar{D}p_0^2 e^{-4\tau} (1 + 2f - p_0^2 e^{-6\tau})] \\ &\quad \times (2f - 1 + p_0^2 e^{-6\tau} + 4Ne^{-\tau})^{-1}, \\ b(\tau) &= Ne^{-2\tau} (4 + \bar{D}p_0^2 e^{-4\tau}) (2f - 1 + p_0^2 e^{-6\tau} + 4Ne^{-\tau})^{-1}, \\ c(\tau) &= (\bar{D}/N)p_0^2 e^{-2\tau} (p_0^2 e^{-6\tau} - 1 - 2f), \quad d(\tau) = -\bar{D}p_0^2 e^{-4\tau}, \end{aligned} \quad (28)$$

which determines the stability of the thread. The problem is controlled by only two dimensionless parameters

$$\bar{D} = \frac{D}{\dot{\epsilon} h_0^2}, \quad N = \frac{h_0 \bar{n} k_B T}{\gamma}. \quad (29)$$

We are interested in the stability of the thread for small h_0 , which means that we can neglect $b(\tau)$ and all terms proportional to N , which scale like h_0 . Now (27) can be solved in the form

$$\epsilon_1 = \epsilon_1^{(0)} e^{\int_0^\tau a(\tau') d\tau'}, \quad \epsilon_4 = \epsilon_4^{(0)} \exp\{\bar{D}p_0^2 (e^{-4\tau} - 1)\} + \int_0^\tau c(\tau') \epsilon_1(\tau') d\tau'. \quad (30)$$

In the limit of small h_0 , the growth of ϵ_1 is controlled by the eigenvalue

$$\omega = a(\tau) \approx 2\bar{D}p_0^2 e^{-4\tau} \frac{1 + 2f - p_0^2 e^{-6\tau}}{2f - 1 + p_0^2 e^{-6\tau}}, \quad (31)$$

so that growth occurs in the long-wavelength limit, for initial wave numbers $k_0 \lesssim \sqrt{1 + 2f} h_0^{-1}$. It is clear from (31) that the behavior of ω remains essentially unchanged, as long as its value is not too far from the value $f = 2$ predicted by slender jet theory.⁷ In the absence of a better estimate, we will assume $f = 2$ for the calculations to be reported below.

As an aside, we note that for vanishing \bar{D} , $a(\tau)$ becomes positive in the limit $p_0 \rightarrow \infty$, corresponding to instability at very small wavelengths. This is clearly unphysical, and represents a failure of the slender jet description in this limit. We therefore ignore this branch of solutions, as it is not related to the polymer concentration becoming non-uniform. Rather, it represents an apparent instability of the Oldroyd B model, which is expected to be cured in a fully three-dimensional description. It would be interesting to perform such a stability analysis, along the lines of Ref. 27, but using an exponentially thinning thread as the base solution.

Significant growth occurs when $\bar{D} \gtrsim 1$, in other words when h_0 is in the order of the critical radius

$$h_{cr} = \sqrt{D/\dot{\epsilon}}. \quad (32)$$

Owing to the exponential time dependence of some of its coefficients, $a(\tau)$ eventually becomes negative and the perturbation ϵ_1 returns to zero. The reason is that perturbations stretch to increasingly long wavelengths, and transport becomes inefficient. However, before this happens ϵ_1 grows transiently, as shown in Fig. 2 for a moderate value of $\bar{D} = 2$. As h_0 decreases, the maximum value reached by ϵ_1 increases very rapidly, as we will now show.

To estimate the growth of ϵ_1 , note that its maximum occurs at a time τ_m for which $a(\tau_m) = 0$. In the limit of $\bar{D} \rightarrow \infty$, τ_m increases, and exponentially damped terms in the expression for $a(\tau)$ can be dropped. Thus to leading order, and using the marginal value $p_0^2 = 5$, one obtains

$$\tau_m \approx -\frac{1}{4} \ln\left(\frac{3}{50\bar{D}}\right).$$

Putting $N = 0$ in the expression for $a(\tau)$, the integral (30) can be performed easily in elementary terms, and upon inserting τ_m , we find

$$\epsilon_1^{(\max)} \approx \frac{1.028}{\bar{D}^{1/4}} e^{1.877\bar{D}}. \quad (33)$$

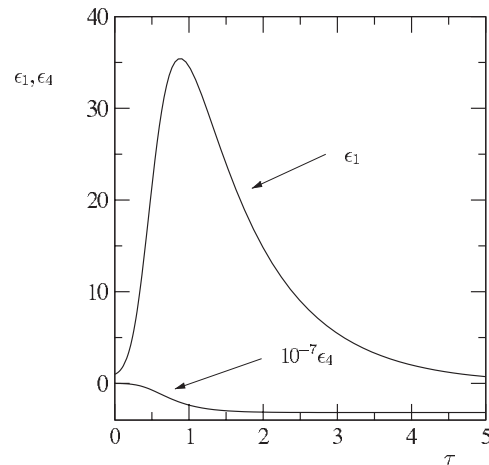


FIG. 2. Growth of perturbation amplitudes according to (27) for $h_0 = 0.5 \mu\text{m}$, which corresponds to $\bar{D} = 2$, $N = 10^{-5}$. The initial reduced wavenumber is $p_0 = \sqrt{5}$. The perturbation to the concentration saturates at -3.17×10^7 .

The constants can be expressed in terms of elementary, yet somewhat cumbersome expressions, which we omit here. For $\bar{D} = 2$, this yields $\epsilon_1^{(\text{max})} = 36.9$, in good agreement with Fig. 2. Since \bar{D} scales like $1/h_0^2$, this maximum value $\epsilon_1^{(\text{max})}$ increases very rapidly with decreasing h_0 . Hence in practice the thread will be observed to be unstable.

The amplitude ϵ_4 of the concentration fluctuations reaches even higher values, as seen in Fig. 2, and the perturbation does not decay in the long time limit, but goes to a constant. The reason is that the growth of ϵ_4 is proportional to the *integral* over ϵ_1 , multiplied by $c(\tau)$, the latter being proportional to h_0^{-3} , which becomes very large. In the long time limit, both $c(\tau)$ and $\epsilon_1(\tau)$ go to zero, so ϵ_4 saturates at a value of

$$\epsilon_4^\infty = \int_0^\infty c(\tau)\epsilon_1(\tau)d\tau. \quad (34)$$

The first contribution to ϵ_4 , which is proportional to $\epsilon_4^{(0)}$, comes from the diffusive term. It decays very quickly with time as the perturbation is stretched, and thus does not lead to decay of ϵ_4 . The typical behavior of ϵ_4^∞ is shown in Fig. 3, the integral having been performed numerically. The expression for $c(\tau)$ in (28) is proportional to \bar{D} , which can be traced back the density–stress coupling coefficient D in (1). This confirms that it is this coupling which is responsible for the giant growth of polymer density fluctuations.

The parameters used for Figs. 2 and 3 were estimated on the basis of some recent experiments^{1,9} performed with semi-dilute solutions of long, flexible polymers (PEO with molecular weight $M_w = 4 \times 10^6$). The polymer time scale is $\lambda \approx 4.3 \times 10^{-2}$ s, and $\gamma/(\bar{n}k_B T) \approx 4.9$ cm. To estimate the diffusion constant D of PEO in water, we used molecular dynamics simulations of much smaller molecules,²⁸ and assumed the diffusion constant to scale like the inverse square root of molecular weight. This results in the value $D \approx 4 \times 10^{-8}$ cm²/s; light scattering experiments²⁹ yield similar results.

Figure 2 shows the solution curves for $h_0 = 0.5 \mu\text{m}$, obtained by integrating the linear system (27) with coefficients (28). As the initial reduced wave number, we chose $p_0 = \sqrt{5}$, the limiting value for growth in the limit $h_0 \rightarrow 0$. The approximate solution (30) (obtained for $N = 0$) is so close that it is indistinguishable on the scale of the figure. Note that while the transient growth of ϵ_1 is still only moderate, concentration fluctuations grow by more than 7 orders of magnitude and do not decay. Also note that the signs are opposite, which means that polymer concentration is *high* at minima of the thread radius. This comes from the fact that polymers are stretched in the extensional flow at the minima, which drives a flux of polymers toward these regions. Figure 3 shows the growth of the asymptotic value (34) of ϵ_4 . The integral was performed numerically, using an analytical

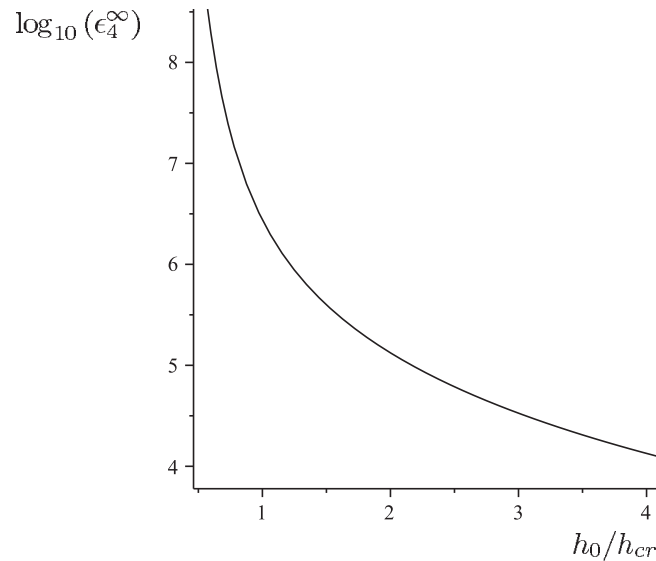


FIG. 3. The logarithm of the long-time value of the amplitude ϵ_4 , as function of h_0/h_{cr} , using the same parameters as for Fig. 2.

expression for $\epsilon_1(\tau)$. Note the extremely rapid growth as h_0 falls below the critical radius h_{cr} , so for all practical purposes ϵ_4 can be considered as growing without limit.

V. DISCUSSION

We have found a novel mechanism for the instability of a highly stretched polymeric thread, which is consistent with the experimental observation of sinusoidal growth of perturbations. Although the growth is transient, the perturbation amplitude can grow over many orders of magnitude, and in the case of concentration fluctuations, does not decay. One should keep in mind that linear theory only describes the initial stages of the instability, until nonlinear effects take over, leading for example to beads with threads attaching them. Thus in practice, significant transient growth may well be indistinguishable from unlimited exponential growth. As a result of the instability, the polymer concentration becomes high in the neck regions, which ultimately form threads between tiny droplets of fluid. This finding is consistent with the experimental observation that threads become highly concentrated with polymer, which ultimately solidifies.¹

Our calculation leads to the identification of a critical thread radius (32), below which coupling between stress and density becomes significant. Since the growth rate increases like h_0^{-2} , the instability will appear quite suddenly, once the threshold has been passed. As growth occurs for wavelengths $\lambda \gtrsim 2.8h_0$, with the wavelength increasing in time, the observed wavelength will be several times the thread radius, as observed experimentally.^{1,9} Instability based on the Rayleigh-Plateau mechanism, on the other hand, predicts a wavelength more than a hundred times the radius.⁹

Calculations have been based on a simple model of dilute, linear Hookean springs, with beads attached to them. In the experiments considered by us,^{1,8,9} polymers are at a semidilute concentration, and obviously their configuration is highly stretched. We expect that while the same coupling terms between the fields are present, the value of the coupling coefficients will be changed owing to nonlinear effects. As a result, there will be more independent parameters, since for example diffusion and transport in (1) are not necessarily controlled by the same Onsager coefficient D , as it is found for the Hookean dumbbell and Rouse models. As remarked in Ref. 14, a nonlinear theory would probably renormalize the two coefficients differently. In particular, if interactions between polymers are taken into account, the coupling between density and stress is expected to be stronger than the mechanism based on diffusion alone, which was assumed in Sec. II. This means the instability could set in at a critical radius somewhat greater than predicted by (32), as observed in experiment.

Otherwise there would not be a significant change in the results, since a different value of, e.g., the stress-density coupling would be dwarfed by growth of the density fluctuations, predicted to be over seven orders of magnitude.

ACKNOWLEDGMENTS

This research was inspired by conversations with Howard Stone during a visit to Princeton. I am grateful to Alexander Morozov and to Tanniemola Liverpool for generously sharing their insight into polymer models, and to Suzanne Fielding and Christian Wagner for discussions and comments on the paper.

- ¹R. Sattler, C. Wagner, and J. Eggers, "Blistering pattern and formation of nanofibers in capillary thinning of polymer solutions," *Phys. Rev. Lett.* **100**, 164502 (2008).
- ²J. Eggers, "Universal pinching of 3D axisymmetric free-surface flow," *Phys. Rev. Lett.* **71**, 3458 (1993).
- ³J. Eggers and E. Villermaux, "Physics of liquid jets," *Rep. Prog. Phys.* **71**, 036601 (2008).
- ⁴A. V. Bazilevskii, S. I. Voronkov, V. M. Entov, and A. N. Rozhkov, "Orientational effects in the decomposition of streams and strands of diluted polymer solutions," *Sov. Phys. Dokl.* **26**, 333 (1981).
- ⁵Y. Amarouchene, D. Bonn, J. Meunier, and H. Kellay, "Inhibition of the finite-time singularity during droplet fission of a polymeric fluid," *Phys. Rev. Lett.* **86**, 3558 (2001).
- ⁶C. Wagner, Y. Amarouchene, D. Bonn, and J. Eggers, "Droplet detachment and satellite bead formation in visco-elastic fluids," *Phys. Rev. Lett.* **95**, 164504 (2005).
- ⁷C. Clasen, J. Eggers, M. A. Fontelos, J. Li, and G. H. McKinley, "The beads-on-string structure of viscoelastic jets," *J. Fluid Mech.* **556**, 283 (2006).
- ⁸M. S. N. Oliveira and G. H. McKinley, "Iterated stretching and multiple beads-on-a-string phenomena in dilute solutions of high extensible flexible polymers," *Phys. Fluids* **17**, 071704 (2005).
- ⁹R. Sattler, S. Gier, J. Eggers, and C. Wagner, "The final stages of capillary break-up of polymer solutions," *Phys. Fluids* **24**, 023101 (2012).
- ¹⁰J. Li and M. A. Fontelos, "Drop dynamics on the beads-on-string structure of viscoelastic jets: A numerical study," *Phys. Fluids* **15**, 922 (2003).
- ¹¹H.-C. Chang, E. A. Demekhin, and E. Kalaidin, "Iterated stretching of viscoelastic jets," *Phys. Fluids* **11**, 1717 (1999).
- ¹²R. B. Bird, R. C. Armstrong, and O. Hassager, *Dynamics of Polymeric Liquids, Volume I: Fluid Mechanics; Volume II: Kinetic Theory* (Wiley, New York, 1987).
- ¹³P. P. Bhat, S. Appathurai, M. T. Harris, M. Pasquali, and G. H. McKinley, "Formation of beads-on-a-string structures during break-up of viscoelastic filaments," *Nat. Phys.* **6**, 625 (2010).
- ¹⁴E. Helfand and G. H. Fredrickson, "Large fluctuations in polymer solutions under shear," *Phys. Rev. Lett.* **62**, 2468 (1989).
- ¹⁵J. W. van Egmond, D. E. Werner, and G. F. Fuller, "Time dependent small angle light scattering of shear induced concentration fluctuations in polymer solutions," *J. Chem. Phys.* **96**, 7742 (1992).
- ¹⁶J. W. van Egmond and G. F. Fuller, "Concentration fluctuation enhancement in polymer solutions by extensional flow," *Macromolecules* **26**, 7182 (1993).
- ¹⁷S. T. Milner, "Dynamical theory of concentration fluctuations in polymer solutions under shear," *Phys. Rev. E* **48**, 3674 (1993).
- ¹⁸A. B. Bhave, R. C. Armstrong, and R. A. Brown, "Kinetic theory and rheology of dilute, nonhomogeneous polymer solutions," *J. Chem. Phys.* **95**, 2988 (1991).
- ¹⁹M. Cromer, M. C. Villet, G. H. Fredrickson, and L. G. Leal, "Shear banding in polymer solutions," *Phys. Fluids* **25**, 051703 (2013).
- ²⁰H. C. Öttinger, "Incorporation of polymer diffusivity and migration into constitutive equations," *Rheol. Acta* **31**, 14 (1992).
- ²¹A. N. Beris and V. G. Mavrantzas, "On the compatibility between various macroscopic formalisms for the concentration and flow of dilute polymer solutions," *J. Rheol.* **38**, 1235 (1994).
- ²²V. G. Mavrantzas and A. N. Beris, "Modelling the rheology and flow-induced concentration changes in polymer solutions," *Phys. Rev. Lett.* **69**, 273 (1992).
- ²³A. W. El-Kareh and L. G. Leal, "Existence of solutions for all Deborah numbers for a non-Newtonian model modified to include diffusion," *J. Non-Newtonian Fluid Mech.* **33**, 257 (1989).
- ²⁴R. G. Larson, *The Structure and Rheology of Complex Fluids* (Oxford University Press, Oxford, 1999).
- ²⁵V. M. Entov and E. J. Hinch, "Effect of a spectrum of relaxation times on the capillary thinning of a filament of elastic liquids," *J. Non-Newtonian Fluid Mech.* **72**, 31 (1997).
- ²⁶V. Tiratmadja, G. H. McKinley, and J. J. Cooper-White, "Drop formation and breakup of low viscosity elastic fluids: Effects of molecular weight and concentration," *Phys. Fluids* **18**, 043101 (2006).
- ²⁷S. L. Goren and M. Gottlieb, "Surface-tension-driven breakup of viscoelastic driven threads," *J. Fluid Mech.* **120**, 245 (1982).
- ²⁸H. Lee, R. M. Venable, A. D. MacKerell, Jr., and R. W. Pastor, "Molecular dynamics studies of polyethylene oxide and polyethylene glycol: Hydrodynamic radius and shape anisotropy," *Biophys. J.* **95**, 1590 (2008).
- ²⁹D. Bonn, Y. Couder, P. H. J. van Dam, and S. Douady, "From small scales to large scales in three-dimensional turbulence: The effect of diluted polymers," *Phys. Rev. E* **47**, R28 (1993).